International Journal of GEOMATE, June, 2017, Vol.12 Issue 34, pp. 32-37
Geotec., Const. Mat. & Env., ISSN:2186-2990, Japan, DOI: http://dx.doi.org/10.21660/2017.34.2660

SHEAR ZONE DEVELOPMENT AND FRICTIONAL INSTABILITY OF FAULT GOUGE

*Momoko Hirata[1], Jun Muto[1], and Hiroyuki Nagahama[1]

[1]Faculty of Science, Tohoku University, Japan

* Corresponding Author, Received: 15 June 2016, Revised: 26 July 2016, Accepted: 30 Nov. 2016

ABSTRACT: Earthquakes are typical phenomena of frictional slip of geomaterials in nature. To evaluate slip instability, shear development in a gouge layer or fault material has been investigated. However, the quantitative relationship between slip instability and shear development has not been revealed because of difficulty in quantitative observation of microstructures under high pressure. Hence, we aim to describe shear development in a gouge layer energetically, and discuss the relation between shear development and slip instability. To this end, we calculated shear angles by utilizing experimental data of gouge. As a result, this study reveals that shear bands in a gouge layer develop at lower angles or almost parallel to rock-gouge boundaries toward the occurrence of unstable slip, particularly under low confining pressure. Additionally, variation in Riedel shear angles throughout gouge layers depends on confining pressures: Under low confining pressures, heterogeneous localized shears trigger voluntary increase in strain. On the other hand, under a high confining pressure, gouge layers deform homogeneously, and the whole of samples slips dynamically. Clarification of shear development of geomaterials is useful for evaluating the occurrence of frictional slip such as earthquakes and slope failures.

Keywords: Frictional slip, Earthquake, Slip instability, Shear development, Fault gouge

1. INTRODUCTION

Earthquakes and slope failures are typical phenomena of frictional instability of geomaterials in nature. Frictional slip often leads to serious physical damage to our society (e.g., humans, society, and infrastructures). In general, frictional slip can be categorized into two types: stable slip and unstable slip. The former is a stationary motion without stress drop, and the latter is accompanied with dynamic stress drop. To prevent or mitigate damages of unstable slip (i.e., earthquakes or slope failures), evaluation for the occurrence of unstable slip is significantly important. With respect to earthquakes, various researchers have tackled on the evaluation of fault instability based on laboratory experiments of rock friction. They proposed (1) evaluation for fault instability by a friction parameter $a - b$ [1]–[3] and (2) importance of fault gouge generated by a repetition of fault slip [4]–[15].

Friction parameter $a - b$ is generally derived from the empirical law called rate and state dependent friction law, and slip instability is discussed with a spring-slider model [1]–[3]. The positive values of the friction parameters lead to stable slip (velocity strengthening), and the negative values of the friction parameters lead to unstable slip (velocity weakening).

With respect to fault gouge, shear zone development in a gouge layer has been focused to assess slip instability. Particularly, transition from the oblique R1-shears formed after peak stress to Y-shears developed parallel to rock-gouge boundaries seems to trigger unstable slip [9], [12]. Gu and Wong [11] also shows that degrees of R1-shears to rock-gouge boundaries progressively decrease with shear. Based on these observations, Ikari et al. [14] empirically proposed possibility for the change in the friction parameter of rock with shear.

Generally, quantitative observation of shear development in deformed granular materials under high pressures is significantly difficult. However, Rowe [16] proposed an index to describe deformation process of granular materials (e.g., glass and quartz) based on their energy ratio composed by stress and strain. The index (i.e., the energy ratio) also can be represented by an internal friction angle which can be related to a coefficient of friction. Because the internal friction angle can also be related to angles of shear planes developed in granular materials, slip instability of simulated fault gouge with shear zone development could be assessed by the energy ratio [17].

Therefore, in this paper, we aim to clarify quantitatively the process of shear zone development toward the occurrence of unstable slip, and to discuss the relationship between slip instability and shear zone development energetically. As a result of our friction experiments with simulated fault gouge, we clarify shear zone development in a gouge layer under high confining pressures quantitatively. Then, we also show possibility for evaluating other unstable slip such as slope failures. This paper is an extended paper of the preliminary paper [18].

2. EXPERIMENTAL ANALYSIS

2.1 Materials and Methods

In this paper, we utilize data of friction experiments with simulated fault gouge published elsewhere [17]. Experiments were conducted by a gas-medium apparatus at confining pressures ranging from 140 to 180 MPa. A sample was composed of gabbroic forcing blocks cut at oblique angle of 50º to the longitudinal axes and simulated fault gouge (quartz gouge). Quartz gouge was sandwiched between two pre-cut gabbroic blocks. Strain gauges were glued onto a gouge layer through Teflon jackets. A set of strain gauges consists of three gauges: one of them crossed a gouge layer (a black strain gauge represented in Fig. 1) and other two were settled at each end of the black strain gauges (blue gauges in Fig. 1). Strains measured by black gauges show deformation of gouge, forcing blocks, and jackets, while strains by blue gauges show deformation of forcing blocks and jackets. Therefore, differences between a black gauge and blue gauges are regarded as deformation of gouge. Three similar sets of gauges were placed on to the gouge layer. Strain gauges measure stress and strain in the major and minor compressive axes; $\sigma_1, \sigma_3, \varepsilon_1$, and ε_3 respectively. For further detail about experimental condition, refer to Hirata et al. [17]. Based on these values, we calculated energy ratio K proposed by Rowe [16] to describe deformation of granular materials using strain rates in both axes $\dot{\varepsilon}_1$ and $\dot{\varepsilon}_3$, as shown in Eq. (1),

$$K = \frac{\sigma_1 \dot{\varepsilon}_1}{2\sigma_3 \dot{\varepsilon}_3}. \quad (1)$$

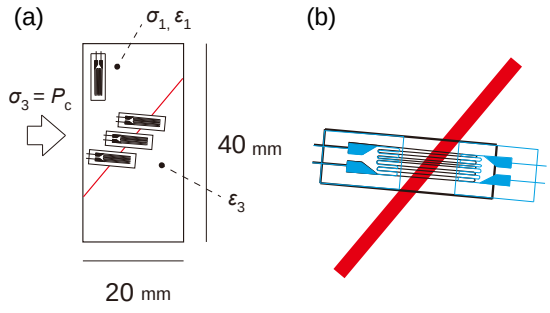

Fig. 1 Schematic diagrams of sample assembly (a) and set of strain gauges (b). A gouge layer was represented as red lines in both (a) and (b). A gauge settled in vertical direction measures $\boldsymbol{\sigma_1}$ and $\boldsymbol{\varepsilon_1}$. The other gauges measure $\boldsymbol{\varepsilon_3}$. The values of $\boldsymbol{\sigma_3}$, confining pressure, regarded as constant in each experiment.

2.1 Experimental Results

From our friction experiments, stress-strain curves with the occurrence of unstable slip were obtained under each confining pressure (Fig. 2).

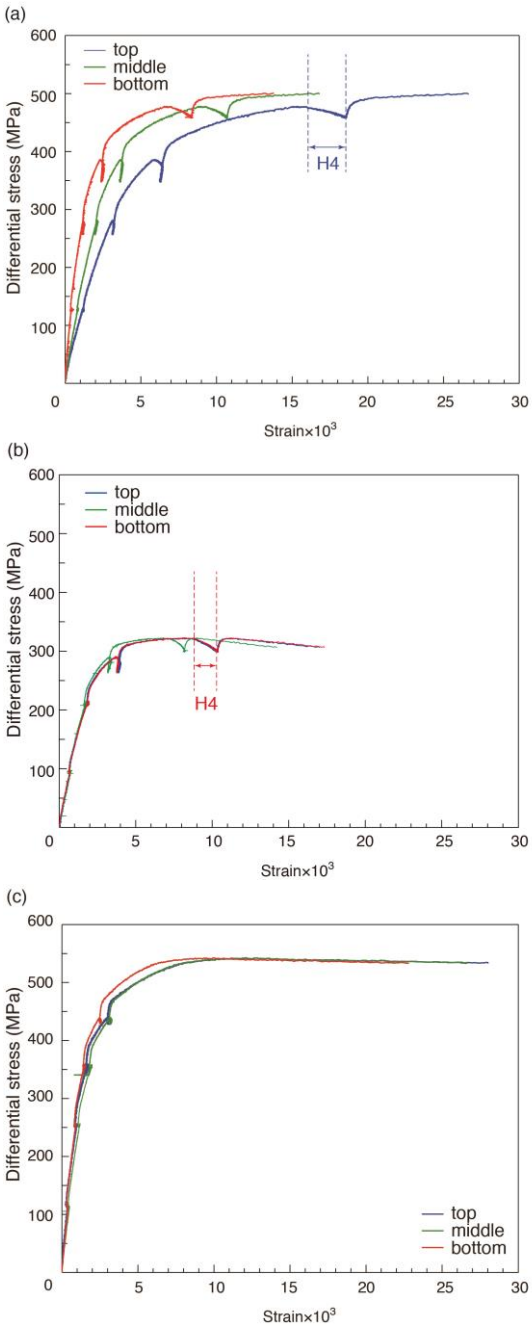

Fig. 2 Stress-strain curves under confining pressures of (a) 140 MPa, (b) 160 MPa, and (c) 180 MPa. Data were obtained from 4th, 3rd, 2nd run experiments with unstable slip, respectively. Colors indicate differential strain gauges: blue, green, and red lines correspond to data of gauges settled at top, middle, and bottom of samples, respectively. In Fig. 2a and 2b, voluntary increase in strain were shown in H4 stages.

Figure 2 can be obtained from multiple loading cycles toward unstable slip. In Fig. 2, elastic deformation of gouge can be confirmed in lower strain. Then, plastic deformation can be recognized in higher strain. The voluntary increases in strain were observed under confining pressures of 140 and 160 MPa although loading was stopped (represented by H4 stage in Fig. 2a and 2b).

The representative change in the energy ratio is shown in Fig. 3. The increase in energy ratios K could be confirmed at all strain gauges until between H1 and H2, between H2 and H3, or between H3 and H4 for top, middle, or bottom strain gauges. Because input energy ($\sigma_1\dot{\varepsilon}_1$) is absorbed into output energy ($2\sigma_1\dot{\varepsilon}_1$) and dissipative energy, increase in energy ratios indicates increase in dissipative energy. Thus, until these early parts of experiments, grain fracture or other phenomena such as reorientation and rearrangement of grains could occur. Moreover, the values of energy ratio varied widely depending on the places where strain gauges were glued. After that, all strain gauges showed decrease toward unstable slip. Especially, the bottom gauge showed the significant reduction in the energy ratio before unstable slip.

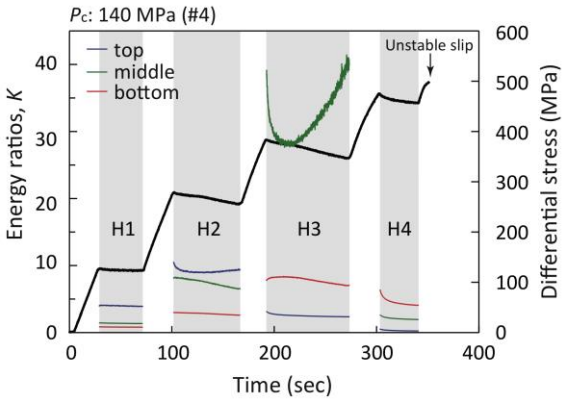

Fig. 3 Change in energy ratios of fault gouge at the 4th run under a confining pressure of 140 MPa. Color legends and the black arrow are same as Fig. 2. Only results of energy ratios at the holding periods were displayed.

The temporal data of energy ratios under each confining pressure is shown in Fig. 4. After the final holding period (H4 stage), all strain gauges showed the significant decreases in energy ratio just before unstable slip. These drops of energy ratio in final stages just before the occurrence of unstable slip (L5 stage) were confirmed under all confining pressures. On the other hand, there were time lags for the sudden sudden drop in K depending on the position of strain gauges. Time lags dec confining pressures: 1.6 or 1.3 seconds at 140 or 160 MPa, respectively.

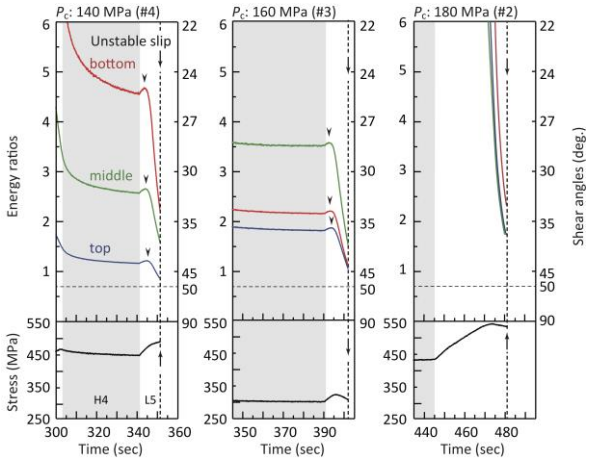

Fig. 4 The temporal data of energy ratios toward unstable slip under confining pressures of 140, 160, 180 MPa. Black marks indicate the beginning of drops in energy ratios at confining pressures of 140 and 160 MPa. Vertical broken lines correspond to the occurrence of unstable slip. Color legends and black arrows are same Figs. 2 and 3. Right vertical axes indicate Riedel shear angles in a gouge layer (see 3.1).

3. DISCUSSION

3.1 Estimates of Riedel Shear Angles

According to [19]–[21], energy ratio expressed as Eq. (1) can be rewritten as follows,

$$K = \tan^2\left(\frac{\pi}{4} + \frac{\phi}{2}\right), \tag{2}$$

where ϕ is the internal friction angle [16], [19]–[21]. Thus, the change in energy ratios observed during our friction experiments indicates the change in internal friction angles. The internal friction angle can also be connected to Riedel shear (e.g., R1-shears) angles as in Eq. (3) [5], [22],

$$\theta = \frac{\pi}{4} - \frac{\phi}{2}, \tag{3}$$

where θ is the Riedel shear angles with respect to the major compressive axis. Therefore, Riedel shear angles developed in a gouge layer can be estimated quantitatively based on Eqs. (2) and (3) by utilizing energy ratios. Right vertical axes in Fig. 5 showed the estimated Riedel shear angles. According to Byerlee et al. [5] and Niiseki [21], change in Riedel shear for clockwise direction is taken to be positive. Shear angles of 50º (horizontal broken lines in Fig. 4) correspond to the angle of rock-gouge boundaries. Figure 4 indicates that Riedel shear angles gradually

change with progress of experiments and decrease rapidly just before the occurrence of unstable slip.

Figure 5 illustrates development of Riedel shears in a gouge layer based on the calculations of Riedel shear angles as in Eqs. (2) and (3). Under all confining pressures, at first, Riedel shears develop toward high angles to the rock-gouge boundaries with shear (L1–L3, L1–L2 or L3, and L1–L4 for confining pressure of 140, 160, and 180 MPa, respectively). After that, Riedel shears develop in lower angles to the rock-gouge boundaries toward the occurrence of unstable slip. Particularly, under a confining pressure of 140 MPa, the top of samples shows almost parallel (~ 3°) to the rock-gouge boundary at unstable slip. As a general trend, Riedel shears at the middle part of samples tend to develop at higher angles than those at top parts when unstable slip occurred. In Fig. 5b, Riedel shears at the middle part also develop at a higher angle than that at the bottom part. This development of Riedel shears in low angles near the rock-gouge boundaries is consistent with Gu and Wong [11]. Degrees of internal heterogeneity of gouge structures depend on confining pressures; gouge shows internal heterogeneity of microstructures at a low confining pressure and internal homogeneity of gouge structures at a high confining pressure. This tendency reflects the variety of energy ratios depending on confining pressures as mentioned above.

Let us consider the relationship between microstructural development in a gouge layer and mechanical behaviors of gouge. As shown in Fig. 2, the voluntary increases in strain were confirmed under confining pressures of 140 MPa and 160 MPa, especially at top of a sample under 140 MPa. On the other hand, it could not be confirmed under confining pressure of 180 MPa. Therefore, it is considered that localized shears (e.g., the almost parallel shear to a rock-gouge boundary at top of a sample under a confining pressure of 140 MPa) trigger voluntary slip at lower confining pressures, while the whole of sample with internal homogeneity of gouge structures slides rapidly under high confining pressures. Consequently, in order to occur unstable slip, sufficient (heterogeneous) shear developments are needed under low confining pressures. Under high confining pressures, unstable slip can occur without internal heterogeneity of microstructures. In this study, we cannot clarify the beginning of unstable slip because of technical difficulty of strain gauges. Further works on relationship between shear development and mechanical behaviors of gouge are necessary to understand it clearly.

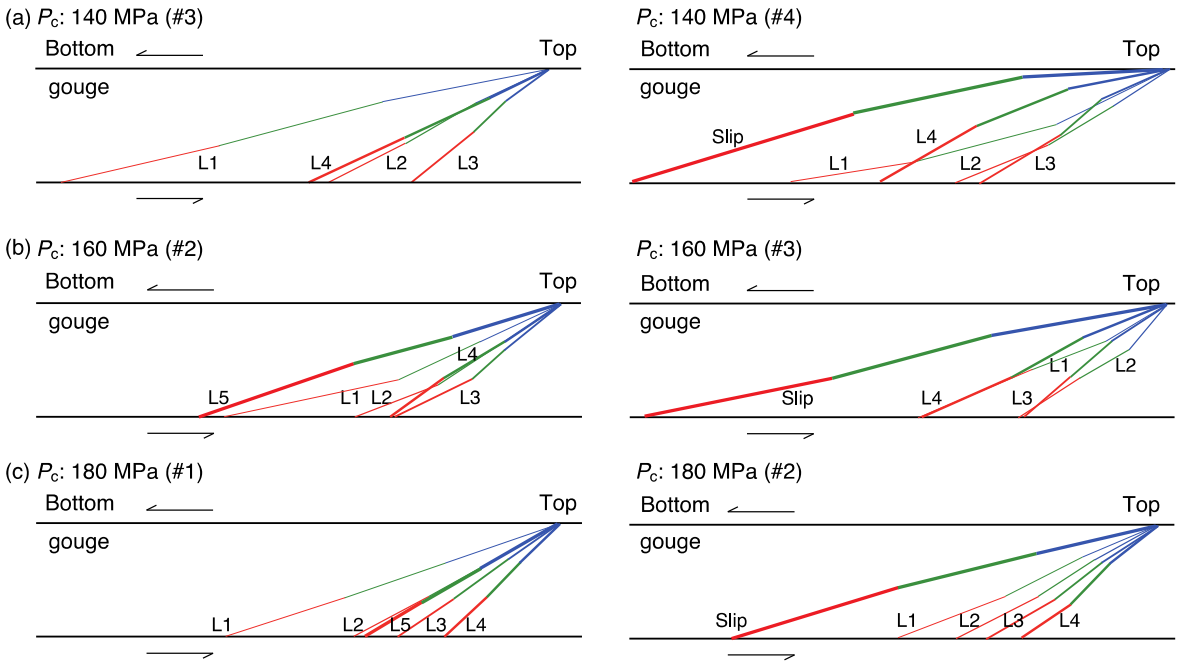

Fig. 5 Development of Riedel shears in a gouge layer under all confining pressures. Estimated Riedel shear angles are represented in top, green, or red lines for top, middle, or bottom of samples, respectively. These lines are obtained at the end of each loading (L1–L5) or at the occurrence of unstable slip. In Fig. 5, they are represented with differential thickness of lines. The right side corresponds to top of samples. The upper or lower receives shear to left side or right side, respectively. The angles mean the differences between Riedel shears and rock-gouge boundaries. These angles are given by $\mathbf{50^\circ - \theta}$.

3.2 Riedel Shear Angles and Energy Ratios

From Eqs. (2) and (3), relationship between Riedel shear angles θ and energy ratios K can be described as follows,

$$\theta = \frac{\pi}{2} - \tan^{-1}\sqrt{K}. \quad (4)$$

According to Hirata et al. [17], energy ratios tend to be larger with confining pressures ($K > 0$). Therefore, Riedel shear angles become smaller with confining pressures. Small values of Riedel shear angles indicate that Riedel shears develop at higher angles to rock-gouge boundaries in our experimental set up. Therefore, as shown in Fig. 5, shear bands develop at higher angles to the rock-gouge boundaries under high confining pressures. On the other hand, shear bands develop at lower angle, or almost parallel to the rock-gouge boundaries under a low confining pressure with progress of experiments.

However, Riedel shear angles depend on not only confining pressure σ_3 but also other factors (i.e., σ_1, $\dot{\varepsilon}_1$, and $\dot{\varepsilon}_3$) because the energy ratio is a function of these four factors as in Eq. (1). With respect to σ_1, the effect of σ_1 on Riedel shear angles can be considered as minor. If Riedel shear angles depend on σ_1 strongly, Riedel shear angles should become similar values in experiments with similar differential stresses (e.g., differential stress of 500 MPa and 450 MPa under confining pressures of 140 MPa and 180 MPa, respectively). Additionally, if Riedel shear angles depend on σ_1, Riedel shear angles become larger with σ_1 based on Coulomb-Navier's failure criterion. However, as shown in Fig. 4, their energy ratios and Riedel shear angles are totally different. In fact, Riedel shear angles are not always increase with differential stress (Fig. 4).

Let us consider the effects of strain rates. In our experimental set up, $\dot{\varepsilon}_1$ took same values regardless of places where gauges settled. On the other hand, $\dot{\varepsilon}_3$ had variations depending on places. This variation in $\dot{\varepsilon}_3$ observed through gauges strongly influences energy ratios as well as Riedel shear angles. Even though samples were applied to under same confining pressures, the values of Riedel shear angles also change (i.e., shears develop heterogeneously) due to variation in $\dot{\varepsilon}_3$. The top of samples under a confining pressure of 140 MPa showed the representative result. Consequently, even though degree of influences on Riedel shear angles is different, Riedel shear angles depend on stress and strain rate in the major and minor compressive axes, respectively.

Internal friction angle is related to plasticity index I_P of soils with water [23]–[26],

$$\phi = \alpha I_P^{-\beta}, \quad (5)$$

where α and β are constants. From Eqs. (2) and (5), evaluation of unstable slip based on energy ratios can take effect of water into consideration. Consequently, through our study, there is quite a possibility that slip instability can be assessed with water effect. Clarification of shear development of geomaterials such as fault gouge can be useful for assessment of the occurrence of earthquakes as well as other fictional slip such as slope failures.

4. CONCLUSION

We investigated Riedel shear development in a gouge layer quantitatively based on energy ratios of fault gouge. From our analysis, it is clear that shears develop at lower angles to rock-gouge boundaries toward unstable slip. Under low confining pressures, gouge shows heterogeneous structures, and localized shear triggers voluntary increase in strain. On the other hand, under a high confining pressure, Riedel shear develops with homogeneous structures thoroughly. To trigger unstable slip under high confining pressures, localized shears are not necessary. The quantitative evaluation of shear development leads to quantitative assessment of fault instability, and will also useful for estimating slip planes of slope failures.

5. ACKNOWLEDGEMENTS

This study was supported by JSPS KAKENHI grant number 15J02421 and Inter-Graduate School Doctoral Degree Program on Science for Global Safety of Tohoku University.

6. REFERENCES

[1] Rice JR and Ruina AL, Stability of steady frictional slipping, J. App. Mech., Vol. 50, Jun. 1983, pp. 343–349.

[2] Ruina A, Slip instability and state variable friction laws, J. Geophys. Res., Vol. 88, Dec. 1983, pp. 10359–10370.

[3] Dieterich JH, Modeling of rock friction: 1. Experimental results and constitutive equations, J. Geophys. Res. Vol. 84, May 1979, pp. 2161–2168.

[4] Scholz CH, Wyss M, and Smith SW, Seismic and aseismic slip on the San Andreas fault, J. Geophys. Res., Vol. 74, Apr. 1969, pp. 2049–2069.

[5] Byerlee J, Mjachkin V, Summers R, and Voevoda O, Structures developed in fault gouge during stable sliding and stick-slip, Tectonophysics, Vol. 44, Jan. 1978, pp. 161–171.

[6] Logan JM, Friedman M, Higgs N, Dengo C, and Shimamoto T, Experimental studies of simulated gouge and their application to studies

of natural fault zones, Proc. Conf. VIII, Analysis of Actual Fault Zones in Bedrock, U. S. Geol. Surv., Open File Rep., 79-1239, 1979, pp. 305–343.
[7] Marone C and Scholz CH, The depth of seismic faulting and the upper transition from stable to unstable slip regimes, Geophys. Res. Lett., Vol. 15, Jun. 1988, pp. 621–624.
[8] Marone C, Raleigh CB, and Scholz CH, Frictional behavior and constitutive modeling of simulated fault gouge, J. Geophys. Res., Vol. 95, May 1990, pp. 7007–7025.
[9] Logan JM, Dengo CA, Higgs NG, and Wang ZZ, Chapter 2 Fabrics of experimental fault zones: Their development and relationship to mechanical behavior, Fault Mechanics and Transport Properties of Rocks, Int. Geophys. Ser., Vol. 51, A Festschrift in Honor of Brace WF, Evans B, and Wong T-f, Ed. Academic Press, 1992, pp. 33–67.
[10] Marone C and Kilgore B, Scaling of the critical slip distance for seismic faulting with shear strain in fault zones, Nature, Vol. 362, Apr. 1993, pp. 618–621.
[11] Gu Y and Wong T-f, Development of shear localization in simulated quartz gouge: Effect of cumulative slip and gouge particle size, Pure Appl. Geophys., Vol. 143, Mar. 1994, pp. 387–423.
[12] Marone C, Laboratory-derived friction laws and their application to seismic faulting, Annu. Rev. Earth Planet. Sci., Vol. 26, May. 1998, pp. 643–696.
[13] Wong T-f, Baud P, and Klein E, Localized failure modes in a compactant porous rock, Geophys. Res. Lett., Vol. 28, Jul. 2001, pp. 2521–2524.
[14] Ikari MJ, Marone C, and Saffer DM, On the relation between fault strength and frictional stability, Geology, Vol. 39, Jan. 2011, pp. 83–86.
[15] Onuma K, Muto J, Nagahama H, and Otsuki K, Electric potential changes associated with nucleation of stick-slip of simulated gouges, Tectonophysics, Vol. 502, Mar. 2011, pp. 308–314.
[16] Rowe PW, The stress-dilatancy relation for static equilibrium of an assembly of particles in contact, Proc. R. Soc. Lond. A, Vol. 269, Oct. 1962, pp. 500–527.
[17] Hirata M, Muto J, and Nagahama H, Experimental analysis on Rowe's stress-dilatancy relation and frictional instability of fault gouges, Episodes, Vol. 37, Dec. 2014, pp. 303–307.
[18] Hirata M, Muto J, and Nagahama H, Clarification of shear zone development in a gouge layer related to slip instability, in Proc. 2nd Int. Conf. on Sci., Eng., Env., 2016, pp. 108–112.
[19] Niiseki S and Satake M, The instruction and consideration of Rowe's principle on the minimum energy ratio, in Proc. 36th Annu. Conf. JSCE, Vol. 3, 1981, pp. 5–6 (in Japanese).
[20] Morinaga K and Niiseki S, Consideration about Rowe's stress-dilatancy relation according to variational method, in Proc. 38th Annu. Conf. JSCE, Vol. 3, 1983, pp. 33–34 (in Japanese).
[21] Niiseki S, Formulation of Rowe's stress-dilatancy equation based on plane of maximum mobilization, in Proc. 4th Int. Conf. Micromech. Granular Media (Powders and Grains), 2001, pp. 213–216.
[22] Morgenstern NR and Tchalenko JS, Microscopic structures in kaolin subjected to direct shear, Géotechnique, Vol. 17, Dec. 1967, pp. 309–328.
[23] Kenny TC, Geotechnical properties of glacial lake clays, J. Soil Mech. Found. Eng. Div., Vol. 85(SM3), Jun. 1959, pp. 67–79.
[24] Voight B, Correlation between Atterberg plasticity limits and residual shear strength of natural soils, Géotechnique, Vol. 23, Jan. 1973, pp. 265–267.
[25] Kanji MA, The relationship between drained friction angles and Atternberg limits of natural soils, Géotechnique, Vol. 24, Dec. 1974, pp. 671–674.
[26] Dewoolkar MM and Huzjak RJ, Drained residual shear strength of some claystones from front range, Colorado, J. Geotech. Geoenviron. Eng, Vol. 131, Dec. 2005, pp. 1543–1551.